Medical Molecular Morphology (2019) 52:226–234
https://doi.org/10.1007/s00795-019-00225-6

ORIGINAL PAPER

Molecular association of FtsZ with the intrabacterial nanotransportation system for urease in *Helicobacter pylori*

Hong Wu[1,2] · Noritaka Iwai[1,3] · Youichi Suzuki[2] · Takashi Nakano[1,2]

Received: 11 March 2019 / Accepted: 15 May 2019 / Published online: 27 May 2019

Abstract

Helicobacter pylori possesses intrabacterial nanotransportation system (*ib*NoTS) for transporting CagA, VacA, and urease within the bacterial cytoplasm, which is controlled by the extrabacterial environment. The route of *ib*NoTS for CagA is reported to be associated with the MreB filament, whereas the route of *ib*NoTS for urease is not yet known. In this study, we demonstrated by immunoelectron microscopy that urease along the route of *ib*NoTS localizes closely with the FtsZ filament in the bacterium. Supporting this, we found by enzyme immunoassay and co-immunoprecipitation analysis that urease interacted with FtsZ. These findings indicate that urease along the route of *ib*NoTS is closely associated with the FtsZ filament. Since these phenomena were not observed in *ib*NoTS for CagA, the route of *ib*NoTS for CagA is different from that of *ib*NoTS for urease. We propose that the route of *ib*NoTS for urease is associated with the FtsZ filament in *H. pylori*.

Keywords *Helicobacter pylori* · FtsZ · Urease · Intrabacterial nanotransportation system · Immunoelectron microscopy

Introduction

Helicobacter pylori possesses an intrabacterial nanotransportation systems (*ib*NoTSs) in the cytoplasm for its important pathogenic factors, such as CagA, urease, and VacA [1–3]. To clarify the mechanism of *ib*NoTS, it is necessary to elucidate its route and related proteins.

In eukaryotic cells, certain types of proteins are transported between intracellular compartments by vesicles, cytoskeletons, and motor proteins [4–7]. For their intracytoplasmic transportation, proteins are translocated through microfilaments [8–10]. In prokaryotic cells, structural fibrous systems, such as MreB [11], FtsZ [12], and crescentin [13], have been identified as prokaryotic homologs of actin, tubulin, and intermediate filaments in eukaryotic cells, respectively. Recently, we have demonstrated that the bacterial cytoskeleton is a possible route of *ib*NoTS, on the basis of our findings by immunoelectron microscopy and the freezing and thawing method [14]. By the method that enabled to observe the bacterial cytoskeletal filament [15], it was shown that the route of *ib*NoTS for CagA was likely to be associated with the MreB filament, which is a bacterial cytoskeletal filament. In addition, it has been reported that the MreB filament does not associate with *ib*NoTS for urease [14]. In contrast, it remains unclear whether the route and factors associated with *ib*NoTS for urease, which is an important pathogenic factor associated with the colonization on gastric mucosa cells, are associated with bacterial cytoskeletal filaments other than the MreB filaments.

In prokaryotic cells, there are filaments other than the MreB filament. The cell division protein FtsZ is one of the bacterial cytoskeletal filaments and its eukaryotic homolog is tubulin. The FtsZ filament has also been well studied and reported to be involved in bacterial cytokinesis. FtsZ plays an important role in the cytoskeletal framework to form a dynamic ringlike structure (Z ring) in the mitotic phase [16–18]. The FtsZ filaments as a protofilaments localize in the cytoplasm, existing on sheet, spiral structure, or dynamic cytoskeletal patterns during the nonmitotic phase of bacterial cells. It is considered to support cell shape, similar to

✉ Hong Wu
wuhong@osaka-med.ac.jp

1 Project Team for Study of Nanotransportation System, Research & development Center, Osaka Medical College, 2-7 Daigaku-machi, Takatsuki, Osaka 569-8686, Japan

2 Department of Microbiology and Infection Control, Osaka Medical College, 2-7 Daigaku-machi, Takatsuki, Osaka 569-8686, Japan

3 Graduate School of Bioscience and Biotechnology, Tokyo Institute of Technology, 4259 Nagatsuta, Midori-ku, Yokohama, Kanagawa, 226-8501, Japan

the eukaryotic actin fiber, which is closely associated with the eukaryotic intracytoplasmic transportation of proteins [19–22]. Morphologically, it was shown by immunofluorescence microscopy that FtsZ forms filamentous structures in a helically arranged pattern and by transmission electron microscopy that gold particles indicating the presence of FtsZ displayed a diffuse distribution in most bacterial strains [23, 24]. *H. pylori* also has a gene homologous to *ftsZ* and is supposed to have such a cytoskeletal fiber or filament [25–27].

The route of *ib*NoTS for CagA is associated with the MreB filament in *H. pylori*, as previously determined by immunoelectron microscopy [14]. The route of *ib*NoTS for urease may also be associated with filaments other than the MreB filament in bacteria, for example, the FtsZ filament. Furthermore, the freezing and thawing method was developed, by which filaments were observed in the bacterial cytoplasm [15], and applied in the study of the MreB filament and CagA [14]. This method makes it possible to observe the route of *ib*NoTS for urease associated with the FtsZ filament similar to that of *ib*NoTS for CagA associated with MreB filament.

In this study, we examined the interaction between urease along the route of *ib*NoTS with the FtsZ filament by the freezing and thawing method and contrast-enhanced double-immunostaining electron microscopy.

Materials and methods

Bacteria and chemicals

The *H. pylori* strain ATCC43504 was used in this study. The bacterial cells were grown in Brucella broth with 5% horse serum (Koujinbaiyo, Saitama, Japan) in a microaerophilic jar containing an AnaeroPack-MicroAero (MGC, Tokyo, Japan) at 37 °C for 24–48 h. *H. pylori* cells were washed in phosphate-buffered saline (PBS, pH 7.2) and collected by centrifugation (3,000 × *g* for 20 min). The resulting bacterial pellet was resuspended at a concentration of approximately 1×10^8 bacteria/mL. The bacterial cells were then suspended in McIlvaine buffer containing 100 mM citric acid monohydrate and 200 mM disodium hydrogen phosphate at pH 5 and 37 °C for 5 or 15 min to observe the beginning or termination of the urease and CagA shift in bacteria.

Antibodies

A rabbit polyclonal antibody and a mouse monoclonal antibody (Austral Biologicals, San Ramon, CA, USA) against *H. pylori* CagA and a mouse monoclonal antibody against *H. pylori* urease subunit A (UreA, Austral Biologicals, San Ramon, CA, USA) were used as the primary antibodies in analysis by immunoelectron microscopy. Anti-FtsZ serum was prepared using peptides composed of *H. pylori* FtsZ sequences as the antigen for immunization. Thirteen-week-old KLH: JW rabbits were immunized with four subcutaneous injections of a peptide mixture solution four times. The total amount of protein injected approximately 2 mg/rabbit. Serum samples were collected 56th day after the injection and used as the anti-FtsZ serum. The entire immunization protocol was performed by Sigma-Aldrich. Anti-FtsZ serum was used as the antibody for immunization. The specificity of the antibody was examined by Western blot analysis and enzyme-linked immune sorbent assay (ELISA) by Sigma-Aldrich. The bacterial FtsZ molecule was detected in a blot from *H. pylori* that was probed with an anti-FtsZ antibody (serum) but not in a blot from the *Escherichia coli* strain NIHJ JC2 (data not shown). However, it was clarified that the anti-FtsZ serum was detected in *H. pylori* by immunofluorescence microscopy and immunoelectron microscopy (data not shown). Therefore, the anti-FtsZ serum was used for immunolabeling in this study. A goat anti-mouse IgG antibody labeled with 5-nm colloidal gold and a goat anti-rabbit IgG antibody labeled with 10-nm colloidal gold (EY Laboratories, San Mateo, CA, USA) were used as the secondary antibodies in immunoelectron microscopy. For the enzyme immunoassay (EIA), a rabbit polyclonal antibody (sera) against *H. pylori* FtsZ, mouse monoclonal antibodies against *H. pylori* UreA (urease), CagA, and VacA (Austral Biologicals, San Ramon, CA, USA) were used as the primary antibodies, and a horseradish peroxidase (HRP)-conjugated goat anti-mouse IgG (STR, Victoria, BC, Canada) antibody was used as the secondary antibodies.

Measurement of FtsZ–urease interaction of *H. pylori* based on EIA

The level of FtsZ–urease interaction of *H. pylori* cells that were treated with McIlvaine buffer at pH 5 for designated periods was quantified by EIA. To measure the amount of the FtsZ–urease interaction, the buffer containing the bacterial cells was centrifuged at 1,400 × *g* for 10 min at 4 °C, and the resulting bacterial cell pellet was harvested and sonicated using a CelLytic™ B Plus Kit (Sigma-Aldrich, St. Louis, MN, USA) to lyse the bacterial cells, followed by centrifugation at 10,000 × *g* for 5 min. The supernatant of the resulting protein lysates was harvested and then prepared for examining the amount of FtsZ–urease interaction of *H. pylori* by EIA. We utilized microwells coated with the polyclonal anti-*H. pylori* FtsZ rabbit antibody (sera). The microwells were incubated at 4 °C for 24 h. After washing with TPBS [0.05% Tween-20 in 150 mM phosphate-buffered saline (PBS, pH 7.2)], Blocker Casein in PBS (Thermo, Tokyo, Japan) was added to the wells to block nonspecific reactions, and then diluted lysate samples were added to the microwells, which

were then incubated for 1 h and then washed with TPBS. A mouse monoclonal anti-UreA antibody (urease) or CagA or VacA was used as a detection antibody. A HRP-conjugated anti-mouse IgG antibody was added to the wells, which was then incubated for 1 h at room temperature. The wells were washed with TPBS to remove any unbound substances. 2,2′-Azino-di-(3-ethyl-benzthiazoline-6-sulfonate) (ABTS, KRL, Gaithersburg MD, USA) was added, and the wells were incubated for another 40 min. A stop solution, 10% sodium dodecyl sulfate (SDS), was added, and absorbance was measured spectrophotometrically at 405 nm.

Co-immunoprecipitation analysis (Co-IP)

One hundred microliters of SureBeads Protein G Magnetic Beads (Bio-Rad, Tokyo, Japan) were washed with TPBS three times using a magnetic stand. Magnetize beads were resuspended with 300 µL of TPBS and mixed with 100 µL of anti-*H. pylori* FtsZ rabbit antibody or control rabbit serum. After incubation at 4 °C for 1 h, 100 µL of *H. pylori* cell supernatant, which had been lysed with a CelLytic B Plus Kit (see above), was added to the bead/antibody mixture, and the reaction was further incubated at 4 °C for 3 h with rotation. The bound complexes were washed three times with 500 µL of TPBS and resuspended in 30 µL SDS sample buffer. Supernatant fraction before the first wash was also collected as input fractions and mixed with same amount of SDS sample buffer.

For immunoblotting analysis, 5 µL of samples (immunoprecipitates) and 2 µL of input fractions were denatured, separated by 10% SDS-PAGE, and transferred to an Immobilon-P transfer membrane (Millipore, Tokyo, Japan). For immunoblotting analysis, the primary antibody was mouse monoclonal anti-UreA antibody, and the secondary antibody was TrueBlot ULTRA anti-mouse IgG conjugated with HRP (Rockland, Limerick, PA, USA). Proteins detected were visualized using the Fusion-FX7 imaging system (Vilber Lourmat, Collégien, France).

Fixation and staining for immunoelectron microscopy

For the analyses of urease or CagA and FtsZ molecular localization in an *H. pylori* cell, *H. pylori* colonies treated at acidic pH described above were fixed with 1% glutaraldehyde in 50 mM cacodylate buffer (pH 7.2) at 4 °C for 60 min. Another sample was subjected to freezing and thawing before fixing to observe the structure of the filaments containing FtsZ filament in bacterial cells, as described previously [15]. The fixed colonies were then embedded in Lowicryl K4M resin (Electron Microscopy Science), which were then cut into ultrathin sections (Sorvall MT-5000, Du Pont) as described previously [1].

The ultrathin sections on a grid were treated with 5% normal goat serum in PBS to block nonspecific reactions. The sections were then double-stained with a mouse antibody against *H. pylori* UreA or CagA and a rabbit antibody against FtsZ in sera (primary antibodies), followed by 5-nm colloidal gold-labeled anti-rabbit IgG and 10-nm gold-labeled anti-mouse IgG-labeled goat antibodies (secondary antibodies). The sections were made to react with the primary antibodies and the secondary antibodies as described previously [1]. Finally, the immunostained sections were subjected to contrast-enhanced staining as described previously [28]. All procedures for contrast enhancement were performed at room temperature.

All the sections were observed under a transmission electron microscope (H-7650 type, Hitachi, Tokyo, Japan). Electron micrographs were taken at a magnification of 5,000–8,000×.

Morphometric and statistical analyses

The number of immunogold particles associated with *H. pylori* cells was determined from the immunoelectron photomicrographs obtained. The visible area of bacterial cells in the photomicrographs was measured using an image analyzer (Image J. NIH, USA), and the number of immunogold particles per unit area was counted in a randomly chosen cytoplasmic area of $7–10 \times 10^6$ nm^2. To quantify the distribution of immunogold particles, the densities of the particles per square micrometer in three portions of a bacterial cell were determined. The principle of dividing an *H. pylori* cell into three portions was described previously [1, 29].

Results

To clarify whether the route of *ib*NoTS for urease is closely associated with the FtsZ molecule, we first examined the colocalization of urease and the FtsZ molecule in bacterial cells treated at an acidic pH for 5 or 15 min by double-immunostaining electron microscopy, since we have reported that the shift of *ib*NoTS for urease from the cytoplasm to the periphery near the bacterial membrane in an acidic pH treatment for 5 and 15 min, respectively. The specific colocalization of FtsZ-immunogold particles (large particles) and urease-immunogold particles (small particles) was observed in *H. pylori* treated at an acidic pH for 5 and 15 min (Fig. 1a, b) on the route of *ib*NoTS for urease. Although the localization of urease was shifted from the cytoplasm to the periphery near the bacterial membrane, the localization of FtsZ was not shifted in bacteria treated at acidic pH for 15 min. These findings suggest that the route of *ib*NoTS for urease is closely associated with the FtsZ molecule.

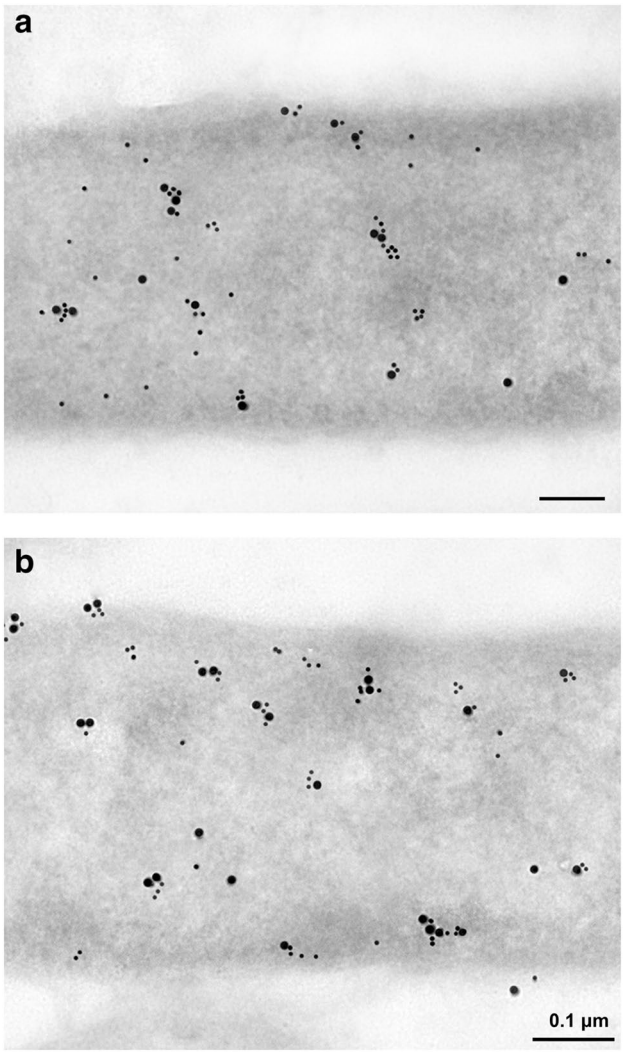

Fig. 1 Localizations of *H. pylori* urease and FtsZ by double-staining immunoelectron microscopy. Relationship between the localizations of urease and FtsZ in *H. pylori* treated with acidic pH medium examined by double-staining immunoelectron microscopy. Large immunogold particles were associated with FtsZ and small particles with urease. At 5 min (**a**) and 15 min (**b**) of acidic pH medium treatment, the urease-immunogold particles in *H. pylori* were localized close to the FtsZ-immunogold particles. Bar = 0.1 μm in all images

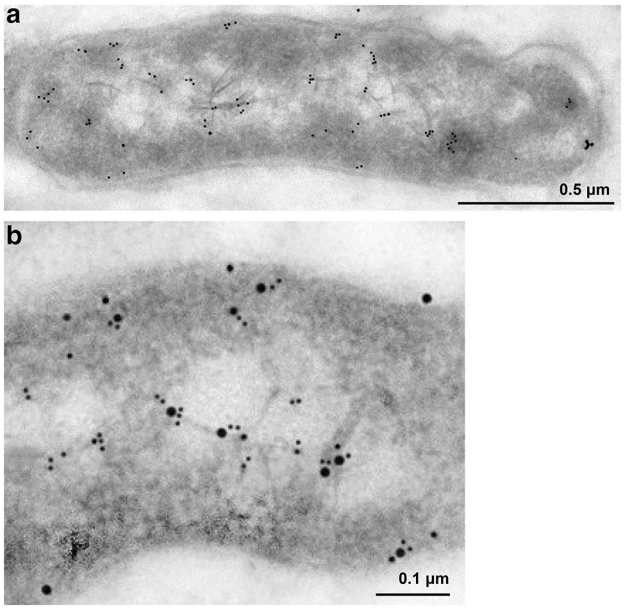

Fig. 2 Localizations of *H. pylori* urease and FtsZ by the freezing and thawing method. **a** Localizations of FtsZ at the filaments of *H. pylori* in nonmitotic phases of bacterial cell. **b** Localizations of urease and FtsZ in acidic-pH-treated *H. pylori* after freezing and thawing determined by double-staining immunoelectron microscopy. Large immunogold particles were associated with FtsZ and small particles with urease. Urease closely localizing with FtsZ was also observed at the filaments of *H. pylori* cells

To confirm whether the route of *ib*NoTS for urease is associated with the FtsZ filament, first, the localization of FtsZ-immunogold particles at the bacterial filament was observed by the freezing and thawing method and immunostaining electron microscopy (Fig. 2a). After the acidic pH treatment for 5 min, the colocalization of urease- and FtsZ-immunogold particles and their relationship with bacterial filaments were observed by double-immunostaining electron microscopy. It was found that some closely colocalized urease- and FtsZ-immunogold particles were observed in the filaments of *H. pylori* cells (Fig. 2b). This finding indicates that the route of *ib*NoTS for urease may be closely associated with the FtsZ filament in *H. pylori* cells.

To confirm whether this close relationship of the route of *ib*NoTS for urease with the FtsZ filament is specific to urease, the relationship of the FtsZ filament with the route of *ib*NoTS for CagA, which is another *ib*NoTS in bacteria, was investigated. First, the localizations of CagA- and FtsZ-immunogold particles were observed by double-immunostaining electron microscopy. No specific colocalization of FtsZ-immunogold particles (large particles) and CagA-immunogold particles (small particle) was observed in *H. pylori* treated at an acidic pH for 5 min when compared with that of urease- and FtsZ-immunogold particles (Fig. 3). These results indicated that FtsZ is not likely to be a molecular scaffold for the route of CagA *ib*NoTS.

To quantitatively validate the stronger association of FtsZ with urease than with CagA, colocalization levels of *H. pylori* FtsZ either with urease or CagA were compared statistically. Among 400 FtsZ-immunogold particles, the number of those found within 30 nm of urease or CagA was counted. It was shown that the number of FtsZ closely associated with urease (Fig. 1a) was twofold higher than that with CagA (Fig. 3), which was significantly different as determined by Student's *t* test ($p < 0.01$, Fig. 4a). Figure 4a' is a schematic diagram of the distance between FtsZ and

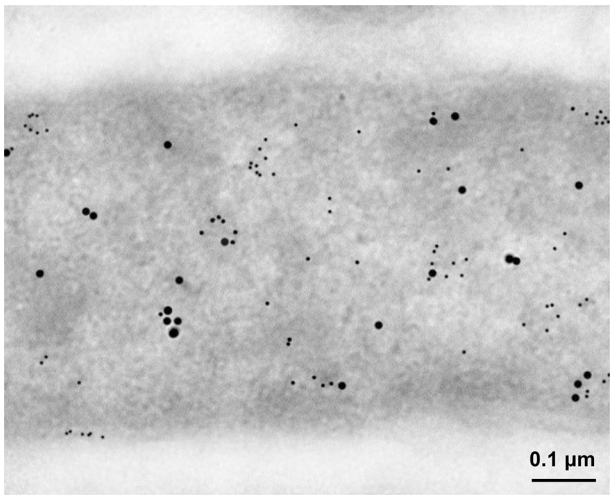

Fig. 3 Localizations of *H. pylori* CagA and FtsZ by double-staining immunoelectron microscopy. Localizations of *H. pylori* CagA and FtsZ. Relationship of the localizations of FtsZ and CagA in *H. pylori* treated with acidic pH determined by double-staining immunoelectron microscopy. Large immunogold particles were associated with FtsZ and small particles with CagA. The CagA-immunogold particles in *H. pylori* treated with acidic pH were not closely localized with the FtsZ-immunogold particles compared with the localizations of urease and FtsZ

urease or CagA. In addition, the density of urease or CagA localized within 30 nm of FtsZ was measured; the density of urease closely associated with FtsZ was also significantly higher than that with CagA ($p < 0.01$, Fig. 4b). Moreover, the overall densities of urease- and CagA-immunogold particles in the bacterial cells were measured and were not found to be significantly different by Student's *t* test (n.s., not significant), but the number of urease- or CagA-immunogold particles found 30 nm from FtsZ was counted and it was shown that the density of CagA was twofold higher than that of urease, which was significantly different as determined by Student's *t* test ($p < 0.01$, Fig. 4c). This indicate that FtsZ closely localized with urease but not with CagA.

The above findings indicate that FtsZ filaments in *H. pylori* cells are not likely to be a molecular scaffold for the route of *ib*NoTS for CagA, but for that of *ib*NoTS for urease.

We next investigated the molecular association of FtsZ with urease by biochemical assays. The lysate of *H. pylori* treated at an acidic pH was examined by EIA. In the EIA, FtsZ–urease complex was first captured by anti-FtsZ sera, and then, urease was detected by using the anti-ureA antibody. When the amount of urease interacted with FtsZ was measured with EIA, a larger amount of urease interacting with FtsZ than of CagA or VacA was detected in *H. pylori* treated at an acidic pH for 15 min (Fig. 5a). Figure 5a' is a schematic of EIA. The difference in optical density (OD) between the two lysates of *H. pylori* was statistically significant as determined by Student's *t* test ($p < 0.01$). The larger amount of urease interacting with FtsZ indicated that urease along the route of *ib*NoTS is closely associated with FtsZ. These findings support the result of immunoelectron microscopy observation, that is, FtsZ in *H. pylori* cells is likely to be a molecular scaffold for the route of *ib*NoTS for urease.

When the lysate of *H. pylori* treated at an acidic pH was also subjected to Co-IP, a higher amount of urease was detected in immunoprecipitates with anti-FtsZ rabbit sera, but not with rabbit control sera (Fig. 5b). The result was consistent with that of EIA indicating FtsZ–urease interaction (Fig. 5a). Therefore, these findings supported the results of immunoelectron microscopy observation, which suggested that FtsZ filaments in *H. pylori* cell were a molecular scaffold for the route of *ib*NoTS for urease.

Discussion

H. pylori urease is essential for gastric colonization and presumably neutralizes acidity, thereby allowing bacterial survival [30]. The pathogenesis of bacterial diseases is explained by the action of exotoxins that are secreted from bacteria, such as CagA by *H. pylori* [31–33], and further extends to other nonsecreted proteins that function in bacterial metabolism, such as urease in *H. pylori* [30, 34, 35]. It has been shown that the intracytoplasmic urease is important for *H. pylori* colonization.

We discovered a new system (*ib*NoTS) of intracytoplasmic transportation of urease in *H. pylori*, and it is considered that the system is closely associated with bacterial colonization and pathogenesis [1]. The system in the transport of important pathogenic factors, such as CagA, urease, and VacA, was demonstrated in *H. pylori* [1–3] and in the transport of cholera toxin in *Vibrio cholerae* [36]. Moreover, the route of *ib*NoTS for CagA is suggested to be separate from that of *ib*NoTS for urease [2], and it has been known that the route of *ib*NoTS for CagA is associated with the MreB filament in *H. pylori* cells, but not that of *ib*NoTS for urease [14]. However, the route of *ib*NoTS for urease has not been clarified in detail.

In this study, we found for the first time that urease closely localized with the FtsZ filament at the start and terminal period of the route of *ib*NoTS for urease. Furthermore, we found that closely localized urease- and FtsZ-immunogold particles observed by double-staining immunoelectron microscopy were associated with the FtsZ filament in *H. pylori* cells. Moreover, CagA did not closely localize to FtsZ-immunogold particles, as determined by double-staining immunoelectron microscopy. These findings indicate that the route of *ib*NoTS for urease is closely associated with the polymerized FtsZ filament, which is among the filaments of *H. pylori*. Furthermore, the close relationship between FtsZ and urease in *ib*NoTS was demonstrated by EIA, in

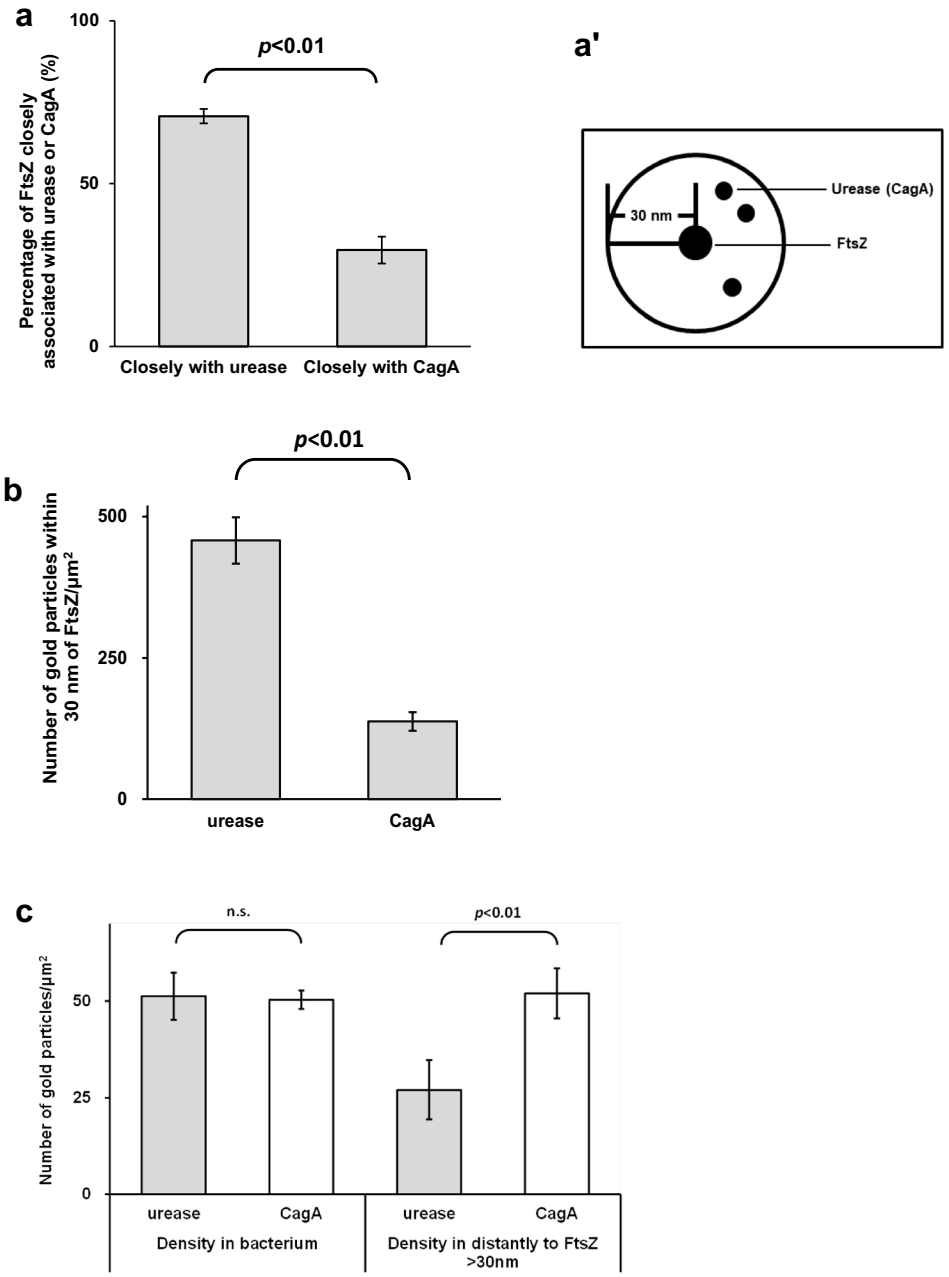

Fig. 4 Analysis of localization of *H. pylori* FtsZ closely associated with urease or CagA. **a** Numbers of FtsZ-immunogold particles close to urease or CagA. The numbers of FtsZ what found within 30 nm from urease or CagA were counted from 400 FtsZ-gold particles. It was shown that the number of FtsZ what closely associated with urease was higher than that associated with CagA, which was significantly different as determined by Student's *t* test ($p < 0.01$). **a'** is a schematic diagram of the distance between FtsZ and urease or CagA. "●" is the image of an immunogold particle. **b** Density of urease or CagA close to FtsZ. The average number of urease or CagA, what localized within 30 nm from FtsZ, was counted; the density of urease closely associated with FtsZ was also significantly higher than that of CagA ($p < 0.01$). **c** Density of urease or CagA far from FtsZ. The average number of urease or CagA localized 30 nm from FtsZ was counted; the density of urease not closely associated with FtsZ was significantly lower than that of CagA ($p < 0.01$), although the average densities of urease and CagA in bacterial cells were not significantly different as determined by Student's *t* test (*n.s.* not significant)

which a high amount of urease colocalizing with FtsZ was confirmed, which was not observed for CagA and FtsZ. The same phenomenon was confirmed by Co-IP.

We have reported an *ib*NoTS-mediated shift of urease to the periphery of the cytoplasm in an acidic extracellular environment, and also demonstrated that the urease did not shift in neutral condition [1]. In this paper, we proposed that the route of *ib*NoTS for urease shifted at the acidic pH condition was associated with the FtsZ filament in *H. pylori*. We found that the route of *ib*NoTS for urease was associated with the FtsZ filament. Since the urease did not shift at the neutral extracellular environment, it was considered that the urease of *H. pylori* treated at neutral pH was not associated with the FtsZ filament. In this study, at the neutral pH treatment, we found that most of the urease was not associated with FtsZ in immunoelectron microscopy analysis. In addition, enzyme immunoassay and co-immunoprecipitation analysis revealed that the urease did not interact with FtsZ (data not shown). Although, in this study, only the ATCC43504 strain of *H. pylori* was used; further studies using other strains of *H. pylori* should be performed in near future.

H. pylori possesses *ib*NoTS for transporting CagA, VacA, and urease toward type IV, V secretion machinery, and UreI,

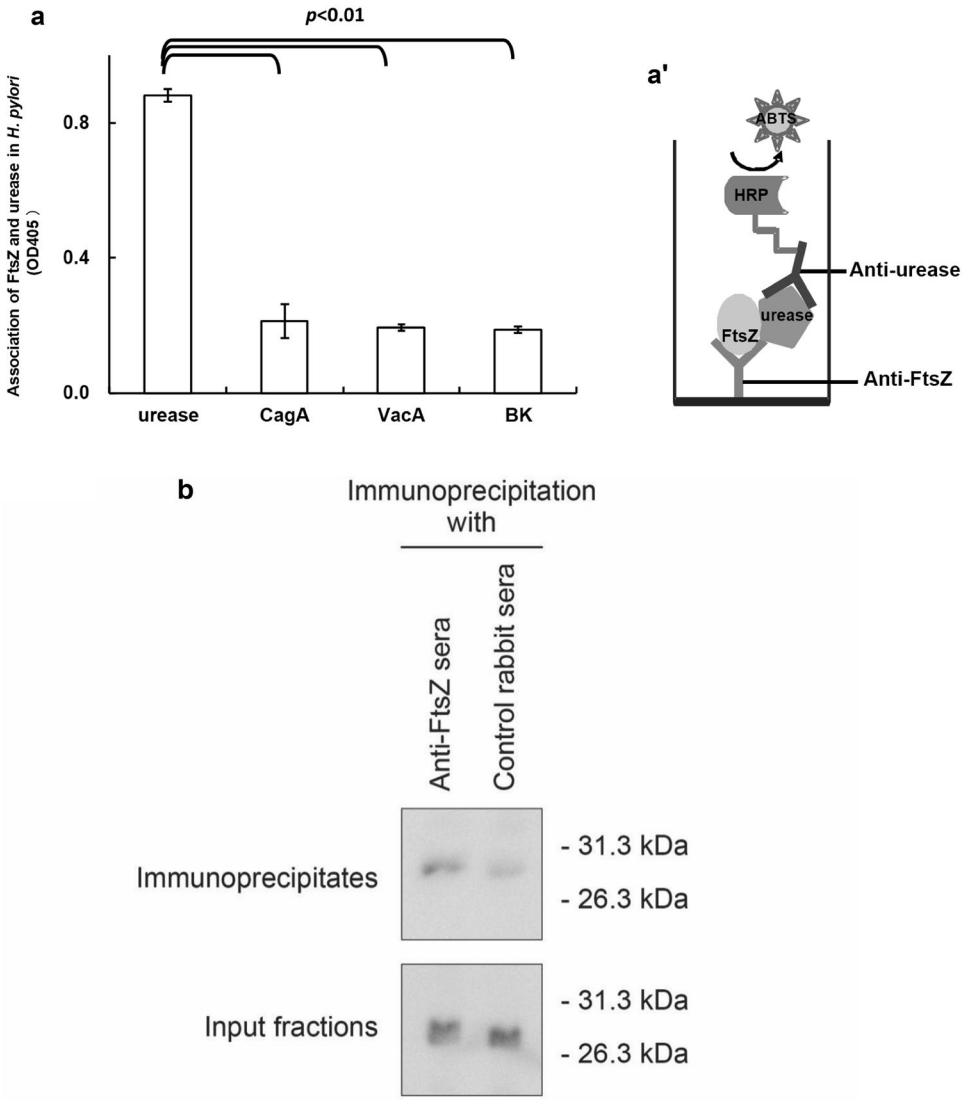

Fig. 5 Amounts of urease interacting with FtsZ in lysate of *H. pylori* determined by EIA and Co-IP. **a** EIA was performed to examine the amount of urease interacting with FtsZ in lysate of *H. pylori*. The amount of urease interacting with FtsZ in *H. pylori* treated at an acidic pH was examined using the rabbit polyclonal anti-FtsZ serum and mouse monoclonal anti-UreA antibody. The amount of urease interacting with FtsZ was higher than that of CagA interacting with FtsZ in the lysate of *H. pylori* ($p < 0.01$; Student's *t* test). BK: background level. **a'** is a schematic of EIA. **b** Co-IP was performed to examine the FtsZ-urease interaction. Supernatant of cell lysate obtained from *H. pylori* treated with an acidic pH was subjected to immunoprecipitation using the rabbit polyclonal anti-FtsZ serum. Immunoprecipitates were separated by SDS-PAGE and blotted on a transfer membrane. Urease in the immunoprecipitates was detected by mouse monoclonal anti-UreA antibody

respectively, at acidic pH [1–3]. These pathogenic factors may have a molecule related to their transport in the cytoplasm of bacterial cells, and the molecule may transport a pathogenic factor to their site of action. Urease is produced in the cytoplasm and transported toward UreI, which exists in the bacterial membrane, by some transport molecules [37, 38]. The transport of urease in the cytoplasm may be through a chemotaxis system in *H. pylori* [39–41]. Our results indicate that urease is transported through FtsZ filament to the bacterial inner membrane where UreI exists. Therefore, the molecules may be FtsZ filament, which localize in the cytoplasm existing on sheet, spiral structure, or dynamic cytoskeletal patterns during the nonmitotic phases of bacterial cells [19–22].

Regarding the route of transport for urease, in this study, we found that urease shifts to a site near the FtsZ filament. The FtsZ filament, which forms the bacterial cytoskeletal fiber [11, 42], is considered to play an important role by providing the cytoskeletal framework to form a dynamic ringlike structure (Z ring) during the mitotic phase of bacterial cells [16–18] and localizes in the cytoplasm existing on sheet, spiral structure, or dynamic cytoskeletal patterns during nonmitotic phases of bacterial cells [19–22], similar to the eukaryotic actin fiber, which closely corresponds to the eukaryotic intracytoplasmic transportation of proteins. *H. pylori* also has a gene homologous to *ftsZ* and is supposed to have such a cytoskeletal fiber or filament [25–27]. From our results, it is highly possible that the transport route for urease is associated with the FtsZ filament. Our fluorescence microscopy and immunoelectron microscopy results indicate that the localization of FtsZ is distributed from the inner membrane to the cytoplasm of bacterial cells (data not shown). It is considered that urease is shifted through the FtsZ filament.

Regarding the transport route for CagA, it has been reported that the route of *ib*NoTS for CagA may be

associated with the MreB filament, which is a bacterial cytoskeletal filament [14]. In this study, we also demonstrated that the FtsZ filament was not associated with the transport route of *ib*NoTS for CagA. These results also indicate that there may be specific transportation systems for specific pathogenic factors in bacteria; for example, the transport route of *ib*NoTS for urease is different from that for CagA, and route of *ib*NoTS for urease and CagA are separate.

With regard to the distribution of the FtsZ filament, there have been many reports, showing that rod-shaped bacteria have the FtsZ protein that forms one of the bacterial cytoskeletal fibers [11, 42] and localizes in the cytoplasm existing on sheet, spiral structure, or dynamic cytoskeletal patterns in the nonmitotic phases of bacterial cells [19–22]. In this study, from the immunoelectron microscopy of FtsZ-immunogold particle distribution in *H. pylori*, we found that the FtsZ-immunogold particles localized in the bacterial cytoplasm during nonmitotic phases and localized in the division site during the mitotic phase of bacterial cells (date not shown).

In conclusion, we found that the route of *ib*NoTS for urease was closely associated with the FtsZ filament. We propose that *H. pylori* possesses an FtsZ-regulated *ib*NoTS for urease but not for CagA, and the route of *ib*NoTS for urease is the FtsZ protofilament in *H. pylori*. By clarifying the mechanism of *ib*NoTS for urease including its route, we may find a new target in the development of a prophylactic agent against *H. pylori* in the gastric mucosa.

Acknowledgements We thank Mr. Yoshihiko Fujioka and Ms. Yukiko Takada of the Department of Microbiology and Infection Control, Osaka Medical College, for their technical help. We also thank Ms. Hiromi Norimitsu for her help in the preparation of the manuscript.

References

1. Hong W, Sano K, Morimatsu S, Scott DR, Weeks DL, Sachs G, Goto T, Mohan S, Harada F, Nakajima N, Nakano T (2003) Medium pH dependent redistribution of the urease of *Helicobacter pylori*. J Med Microbiol 52:211–216
2. Wu H, Nakano T, Daikoku E, Morita C, Kohno T, Lian HH, Sano K (2005) Intrabacterial proton-dependent CagA transport system in *Helicobacter pylori*. J Med Microbiol 54:1117–1125
3. Wu H, Nakano T, Matsuzaki Y, Ooi Y, Kohno T, Ishihara S, Sano K (2014) A new type of intrabacterial nanotransportation system for VacA in *Helicobacter pylori*. Med Mol Morphol 47:224–232
4. Greber UF (2005) Viral trafficking violations in axons: the herpesvirus case. PNAS 102:5639–5640
5. Gerits N, Mikalsen T, Kostenko S, Shiryaev A, Johannessen M, Moens U (2007) Modulation of F-actin rearrangement by the cyclic AMP/cAMP-dependent protein Kinase (PKA) pathway is mediated by MAPK-activated protein kinase 5 and requires PKA-induced nuclear export of MK5. J Biol Chem 282:37232–37243
6. Hehnly H, Stamnes M (2007) Regulating cytoskeleton-based vesicle motility. FEBS Lett 581:2112–2118
7. Klann M, Koeppl H, Matthias Reuss M (2012) Spatial modeling of vesicle transport and the cytoskeleton: the challenge of hitting the right road. PLoS ONE 7:e29645
8. Bohn W, Rutter G, Hohenberg H, Mannweiler K, Nobis P (1986) Involvement of actin filaments in budding of measles virus: studies on cytoskeletons of infected cells. Virology 149:91–106
9. Bucher D, Popple S, Baer M, Mikhail A, Gong YF, Whitaker C, Paoletti E, Judd A (1989) Antigenic analysis and intracellular localization with monoclonal antibodies. J Virol 63:3622–3633
10. De BP, Burdsall AL, Banerjee AK (1993) Role of cellular Actin in human parainfluenza virus type 3 genome transcription. J Biol Chem 268:5703–5710
11. van den Ent F, Amos LA, Lowe J (2001) Prokaryotic origin of the actin cytoskeleton. Nature 413:39–44
12. Bi EF, Lutkenhaus J (1991) FtsZ ring structure associated with divisions in *Escherichia coli*. Nature 354:161–164
13. Ausmees N, Kuhn JR, Jacobs-Wagner C (2003) The bacterial cytoskeleton: an intermediate filament-like function in cell shape. Cell 115:705–713
14. Wu H, Iwai N, Nakano T, Ooi Y, Ishihara S, Sano K (2015) Route of intrabacterial nanotransportation system for CagA in *Helicobacter pylori*. Med Mol Morphol 48:191–203
15. Nakano T, Aoki H, Wu H, Fujioka Y, Nakazawa E, Sano K (2012) Fine visualization of filamentous structures in the bacterial cytoplasm. J Microbiol Meth 90:60–64
16. Li Z, Trimble MJ, Brun YV, Jensen GJ (2007) The structure of FtsZ filaments in vivo suggests a force-generating role in cell division. EMBO J 26:4694–4708
17. Sun SX, Jiang H (2011) Physics of bacterial morphogenesis. Microbiol Mol Biol Rev 75:543–565
18. Loose M, Mitchison TJ (2014) The bacterial cell division proteins FtsA and FtsZ self-organize into dynamic cytoskeletal patterns. Nat Cell Biol 16:38–46
19. Buss J, Coltharp C, Huang T, Pohlmeyer C, Wang SC, Hatem C, Xiao J (2013) In vivo organization of the FtsZ-ring by ZapA and ZapB revealed by quantitative super-resolution microscopy. Mol Microbiol 89:1099–1120
20. Erickson HP, Taylor DW, Taylor KA, Bramhill D (1996) Bacterial cell division protein FtsZ assembles into protofilament sheets and minirings, structural homologs of tubulin polymers. Proc Natl Acad Sci USA 93:519–523
21. Thanedar S, Margolin W (2004) FtsZ exhibits rapid movement and oscillation waves in helix-like patterns in *Escherichia coli*. Curr Biol 14:1167–1173
22. Niu L, Yu J (2008) Investigating intracellular dynamics of FtsZ cytoskeleton with photoactivation singlemolecule tracking. Biophys J 95:2009–2016
23. Margolin W (2005) FtsZ and the division of prokaryotic cells and organelles. Nat Rev Mol Cell Biol 6:862–871
24. Souza Wd (2012) Prokaryotic cells: structural organisation of the cytoskeleton and organelles. Mem Inst Oswaldo Cruz 107:283–293
25. Specht M, Dempwolff F, Schätzle S, Thomann R, Waidner B (2013) Localization of FtsZ in *Helicobacter pylori* and consequences for cell division. J Bacteriol 195:1411–1420
26. Kamran M, Sinha S, Dubey P, Lynn AM, Dhar SK (2016) Identification of putative Z-ring-associated proteins, involved in cell division in human pathogenic bacteria *Helicobacter pylori*. FEBS Lett 590:2158–2171
27. Nishida Y, Takeuchi H, Morimoto N, Umeda A, Kadota Y, Kira M, Okazaki A, Matsumura Y, Sugiura T (2016) Intrinsic characteristics of Min proteins on the cell division of *Helicobacter pylori*. FEMS Microbiol Lett 363:fnw025
28. Hong W, Morimatsu S, Goto T, Sachs G, Scott DR, Weeks DL, Kohno T, Morita C, Nakano T, Fujioka Y, Sano K (2000)

Contrast-enhanced immunoelectron microscopy for *Helicobacter pylori*. J Microbiol Meth 42:121–127
29. Wu H (2016) Optimum number of bacterial cells for examination of localization of intrabacterial nanotransportation system by semiquantitative immunoelectron microscopy. Bull OMC 62:19–23
30. McGowan CC, Cover TL, Blaser MJ (1996) *Helicobacter pylori* and gastric acid: biological and therapeutic implications. Gastroenterology 110:926–938
31. Covacci A, Telford JL, Giudice GD, Parsonnet J, Rappuoli R (1999) *Helicobacter pylori* virulence and genetic geography. Science 284:1328–1333
32. Backert S, Ziska E, Brinkmann V, Zimny-Arndt U, Fauconnier A, Jungblut PR, Naumann M, Meyer TF (2000) Translocation of the *Helicobacter pylori* CagA protein in gastric epithelial cells by a type IV secretion apparatus. Cell Microbiol 2:155–164
33. Backert S, Moese S, Selbach M, Brinkmann V, Meyer TF (2001) Phosphorylation of tyrosine 972 of the *Helicobacter pylori* CagA protein is essential for induction of a scattering phenotype in gastric epithelial cells. Mol Microbiol 42:631–644
34. Scott DR, Weeks D, Hong C, Postius S, Melchers K, Sachs G (1998) The role of internal urease in acid resistance of *Helicobacter pylori*. Gastroenterology 114:58–70
35. Skouloubris S, Thiberge JM, Labigne A, De Reuse H (1998) The *Helicobacter pylori* UreI protein is not involved in urease activity but is essential for bacterial survival in vivo. Infect Immun 66:4517–4521
36. Aoki H, Wu H, Nakano T, Ooi Y, Daikoku E, Kohno K, Matsushita T, Sano K (2009) Nanotransportation system for cholera toxin in *Vibrio cholerae* O1. Med Mol Morphol 42:40–46
37. Weeks DL, Eskandari S, Scott DR, Sachs G (2000) A H^+-gated urea channel: the link between *Helicobacter pylori* urease and gastric colonization. Science 287:482–485
38. Weeks DL, Sachs G (2001) Sites of pH regulation of the urea channel of *Helicobacter pylori*. Mol Microbiol 40:1249–1259
39. Mizote T, Yoshiyama H, Nakazawa T (1997) Urease-independent chemotactic responses of *Helicobacter pylori* to urea, urease inhibitors, and sodium bicarbonate. Infect Immun 65:1519–1521
40. Nakamura H, Yoshiyama H, Takeuchi H, Mizote T, Okita K, Nakazawa T (1998) Urease plays an important role in the chemotactic motility of *Helicobacter pylori* in a viscous environment. Infect Immun 66:4832–4837
41. Scott DR, Marcus EA, Wen Y, Oh J, Sachs G (2007) Gene expression in vivo shows that *Helicobacter pylori* colonizes an acidic niche on the gastric surface. Proc Natl Acad Sci USA 104:7235–7240
42. Shaevitz JW, Gitai Z (2010) The structure and function of bacterial actin homologs. Cold Spring Harb Perspect Biol 2:a000364